ACS OMEGA

http://pubs.acs.org/journal/acsodf

Article

Binding of Anionic Polyacrylamide with Amidase and Laccase under 298, 303, and 308 K: Docking and Molecular Dynamics Simulation Studies Combined with Experiments

Fanglue Wang,* Liwen Zhang, Dongchen Zhang, Xuefeng Wu, and Shengsong Deng

Cite This: *ACS Omega* 2023, 8, 10040−10050

Read Online

ACCESS | Metrics & More | Article Recommendations | Supporting Information

ABSTRACT: Amidase and laccase play a key role in the degradation process of anionic polyacrylamide (HPAM). However, the largest challenge of HPAM enzymatic degradation is whether the enzyme can bind with a substrate for a period of time. Here, the most suitable complexes, namely, Rh Amidase-HPAM-2 and *Bacillus subtilis* (*B. subtilis*) laccase-HPAM-3, were obtained by docking, and they were carried out for molecular dynamics simulation (MDS) under 298, 303, and 308 K. MDS result analysis showed that Rh Amidase-HPAM-2 was the most stable at 298 K mainly due to a salt bridge and a hydrogen bond, and *B. subtilis* laccase-HPAM-3 was the most stable at 298 K mainly due to two electrostatic and hydrogen bonds. The LYS96 in Rh Amidase-HPAM-2 and LYS135 in *B. subtilis* laccase-HPAM-3 had been the most important in their binding process. The binding of Rh Amidase-HPAM-2 and *B. subtilis* laccase-HPAM-3 was optimal at 303 and 298 K, respectively. HPAM was degraded by mixed bacteria, and the optimal conditions were determined to be 308 K, initial pH = 7, and an inoculated dosage of 2 mL. Under these conditions, the degradation ratio reached 39.24%. The effect of parameters on the HPAM degradation ratio followed a decreasing order of temperature > initial pH > inoculated dosage. The HPAM codegradation mechanism was supposed by mixed bacteria according to test data. The mixed bacteria secreted both amidase and laccase, and they interacted jointly with HPAM. These results lay a theoretical foundation to design and modify the enzyme through mutation experiments in the future.

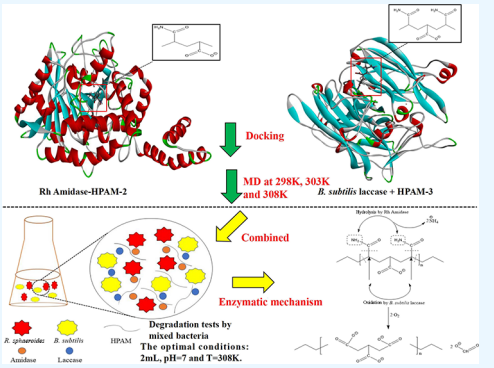

1. INTRODUCTION

Anionic polyacrylamide (HPAM) is a linear polymer flocculant that has been used in clarifying slime water.[1−4] The carboxyl side chain of HPAM is negatively charged in an alkaline environment, and the suspension is clarified by an adsorption bridge.[5] A large amount of HPAM will accumulate in the cycle water of coal dressing, which will reduce the adsorption capacity of coal slime on the flotation reagent.[6] In addition, the emission of coal preparation wastewater containing HPAM can cause wide-scale water pollution.[7] Hence, it is of great significance to transform HPAM into nontoxic substances.

There are many methods for degrading HPAM, including physical degradation,[8] chemical degradation,[9] photocatalytic degradation,[10] and biodegradation.[11] With more and more attention paid to environmental protection and sustainable development, many researchers begin to be apt to biodegradation due to the environmental friendliness, mild condition, and no secondary pollution.[12] Nowadays, dominant strains were obtained through screening from the environment polluted by HPAM for a long time. Wen et al.[13] found two strains *Bacillus cereus* and *Bacillus flexu* from activated sludge and oil soil. They concluded that the bacteria used the amide side chain of HPAM as their nitrogen source. Bao et al.[14] isolated and obtained two strains *Bacillus cereus* and *Bacillus* sp. from polymer flooding-produced water. They found that the amide group of HPAM was hydrolyzed into carboxyl by amidase, and there was a peak at 2.85 min corresponding to polyacrylate (PAA) in HPLC after degradation. Additionally, there was no peak corresponding to acrylamide, indicating that the toxic acrylamide was not produced. PAA is a kind of intermediate metabolite of HPAM and provided a carbon source.[15] The larger PAA fragment was more difficult to be degraded than the smaller ones. According to the difference of starch-cadmium iodide and total organic carbon, the amide side chain was degraded more readily than PAA.[16] The key enzymes detected in the HPAM fermentation broth play an important role in biodegradation.[17] Zhang et al.[12] found that dehydrogenase and urease participated in HPAM degradation. Dehydrogenase promoted electron transfer and oxidation,

Received: November 17, 2022
Accepted: February 28, 2023
Published: March 9, 2023

while urease accelerated the transformation of the amide groups. Song et al.[18] found that the laccase activity was not affected by the concentration of HPAM. They pointed out that the amide group of HPAM was easy to be hydrolyzed by amidase, and PAA, the carbon skeleton of HPAM, was formed. Then, PAA was oxidized by oxygenase. However, the key problem for HPAM degradation is whether the enzyme can combine steadily over time with a substrate. Furthermore, the enzyme isolated from the environment has poor stability, which limits its extensive application.[19]

The formation of the enzyme with the substrate complex is crucial in determining the reaction rate. According to the theory of enzymatic reaction dynamics, the maximum affinity between the enzyme and the substrate indicates that it is the easiest to achieve the maximum reaction rate at a very low substrate concentration. Moreover, the larger the affinity of the enzyme−substrate complex is, the smaller the K_m value is. K_m is a characteristic constant of an enzyme. Hence, the substrate with the maximum affinity is the optimal substrate for this enzyme. In our previous study, it has been proven that the laccase-HPAM-3 and amidase-HPAM-2 acquired the highest affinity,[20] which means that they were the most suitable enzyme−substrate complexes. The protein conformation changes during the simulated time can be studied using molecular dynamics simulation (MDS). By calculating the root-mean-square deviation (RMSD) for backbone atoms and the root-mean-square fluctuation (RMSF) for enzyme residues, the highest flexible regions in protein can be identified. In this study, the binding of the most suitable enzyme−substrate complexes at 298, 303, and 308 K was explored using MDS. However, the combination of the enzyme with HPAM at a time has been reported rarely at the molecular level. This study aims to reveal insights into the mechanistic basis for the degradation process of HPAM.

2. MATERIALS AND METHODS

2.1. Materials. The structural models of HPAM were generated by the Build Polymer tool of Materials Studio 2017 software, and both terminals were sealed with methyl groups.[21] Energy minimization was given by the CHARMm force field, as shown in Figure S1. The 3D crystal structures of amidase[22] (PDB code 3A1I) and laccase[23] (PDB code 1GSK) were determined by experiments, and their binding sites can be found easily. Both the amidase from *Rhodococcus* sp. N-771 (Rh Amidase)[24] and laccase from *Bacillus subtilis* (*B. subtilis* laccase)[25] are downloaded from the PDB web (http://www.pdb.org/pdb/home/home.do). Moreover, these two enzymes had the best resolution. Table S1 lists information about selected enzymes. Before docking, the enzymes were prepared using the Prepare Protein tool in Discovery Studio (DS) 2020 to repair the missing loop regions. Meanwhile, waters and all binding ligands were deleted, and hydrogen was added.[26]

2.2. Docking. Docking can search for the optimal binding conformation of the enzyme with the substrate.[27] It was performed using the semiflexible CDOCKER program in DS 2020,[28] and the accuracy of this procedure had been previously validated.[20] The optimal flexible conformations in active sites were obtained based on high-temperature dynamics, and the first 10 optimal conformations were retained. The docking pose with the highest -CDOCKER_Energy score was used for further analysis. The active site in Rh Amidase was created with coordinates *x*: −20.835, *y*: 6.34554, and *z*: −5.67827 and a radius of 5 Å, while the active site of *B. subtilis* laccase was produced using coordinates *x*: 97.3796, *y*: 61.3005, and *z*: −8.42748 and a radius of 5 Å. Figure S2 shows the active sites of two prepared enzymes. Dock Ligands (CDOCKER) settings are given in Figure S3.

2.3. MDS. MDS can explore the effect of temperature on the enzyme−substrate over time[29,30] and find the residues with the largest fluctuation.[31,32] The most suitable complexes were Rh Amidase-HPAM-2 and *B. subtilis* laccase-HPAM-3, and they were carried out using MDS at 298, 303, and 308 K using the GROMACS software package, version 2021.5[33] implementing the Amber03 force field.[34] In order to make the simulation process closer to reality, we solvated the initial structure in a cubic box of 10 × 10 × 10 nm^3 with a single point charge (SPC) water model,[35] adding sodium ions and chlorine ions to neutralize the system. Then, energy minimization was performed by steepest-decent, and a 1 ns NPT MDS at a constant pressure of 1 atm was carried out to equilibrate the system. Finally, a 50 ns NPT MDS was conducted, and its dynamic trajectory was collected for analysis. RMSD and RMSF values were calculated using GROMACS tools gmx rmsd and gmx rmsf. Meanwhile, the interaction energy and the contribution of residues to their interaction energy were calculated by the Calculate Interaction Energy tool in DS 2020. The total energy was also calculated by the Analyze Trajectory tool in DS 2020. The initial or final conformations of MDS production were visualized and compared using Visual Molecular Dynamics (VMD) software. During the MDS, the cutoff value for van der Waals was set at 1.4 nm, and long-range electrostatic interactions were calculated using a particle mesh Ewald method.[36] The time step was set at 2.0 fs, and other specific parameters were default values. The temperature and the pressure were maintained by a Berendsen thermostat[37] and a Berendsen barostat,[38] respectively. All the above simulations were conducted under the Max-Flow platform.

2.4. Strains and Media. A *Rhodobacter sphaeroides* (*R. sphaeroides*) (ATCC17023) was derived from the China General Microbiological Culture Collection Center, and *B. subtilis* (GIM1.256) was purchased from the Guangdong Microbial Culture Collection Center. HPAM was obtained from the Water Treatment Material Plant (Gongyi, China), and its molecular weight was about 1.2 × 10^7. The basal medium was composed of (L^{-1}) glucose, 10 g; peptone, 10 g; yeast extract, 5 g; beef extract, 5 g; NaCl, 5 g; pH = 7. The solid basal medium was basal medium supplemented with 2% agar. The degradation medium was composed of (L^{-1}) $K_2HPO_4{\cdot}3H_2O$, 1.6 g; $KH_2PO_4{\cdot}3H_2O$, 0.4 g; $CaC1_2$, 0.01 g; $MgSO_4{\cdot}7H_2O$, 0.06 g; NaCl, 0.5 g; trace element solution, 5 mL; HPAM, 500 mg; pH = 7. The trace element solution was composed of (L^{-1}) $CuSO_4{\cdot}5H_2O$, 0.8 g; $ZnSO_4{\cdot}7H_2O$, 1.2 g; $MnC1_2{\cdot}4H_2O$, 1 g; $Fe_2(SO_4)_3$, 0.03 g. These two media were sterilized in an autoclave at 120 °C for 30 min before use.

2.5. HPAM Degradation Experiments. The bacterial solution (2 mL) was inoculated into a 250 mL conical flask containing 100 mL of basal medium and enriched at 303 K for 5 days. Then, the enriched 0.5 mL of bacterial solution was inoculated into a 250 mL conical flask containing 100 mL of basal medium again and cultivated at 303 K for 3 days. After that, 2 mL of bacterial solution was inoculated in the degradation medium with a certain HPAM concentration gradient from 100 to 1200 mg/L for domestication. Each stage was incubated at 303 K with an interval of 300 mg/L for 3 days

https://doi.org/10.1021/acsomega.2c07380
ACS Omega 2023, 8, 10040−10050

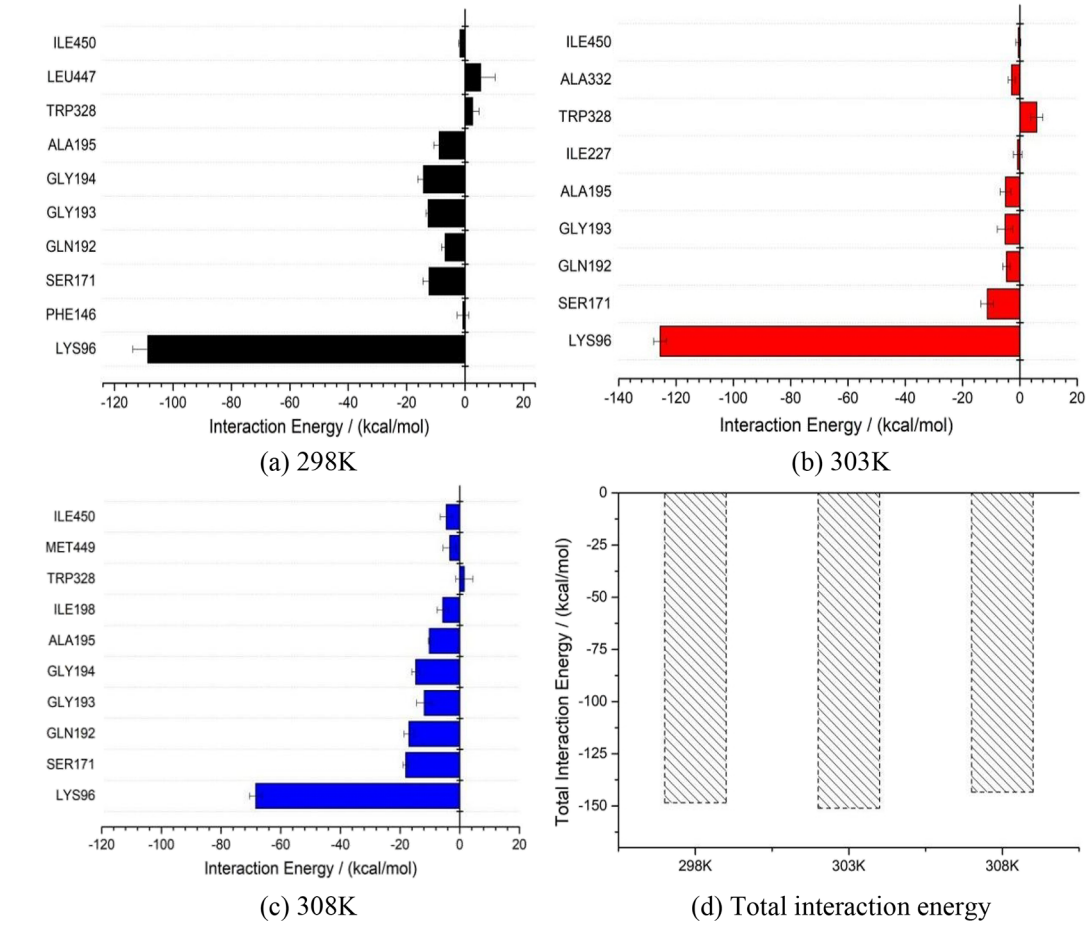

Figure 1. (a–d) Contribution of residues to the interaction energy of Rh Amidase-HPAM-2 and the total interaction energy.

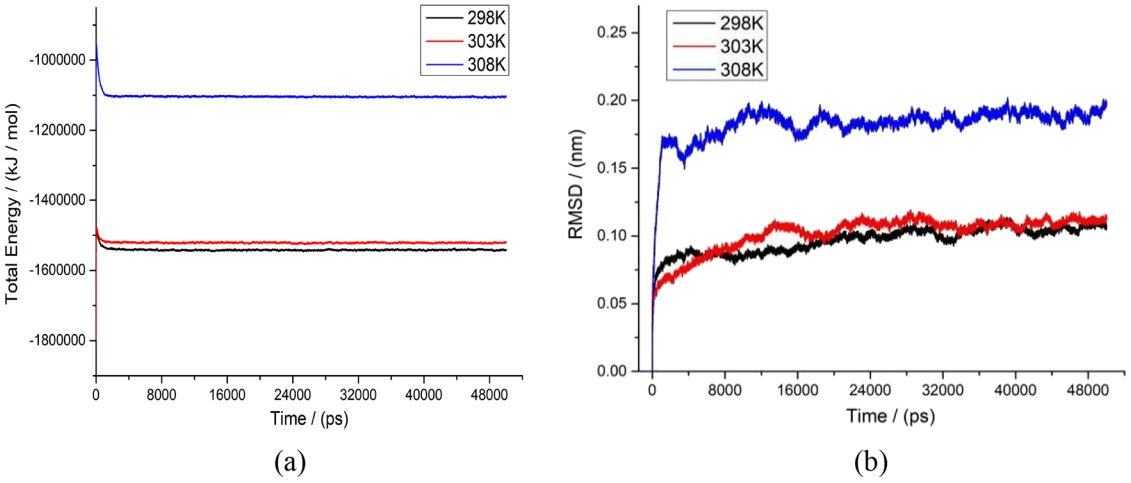

Figure 2. Total energy (a) and RMSD of backbone atoms (b) in Rh Amidase-HPAM-2 under 298, 303, and 308 K.

on an incubator shaker. The strain could be induced to secrete the higher active enzyme by domestication.

The mixed bacteria were obtained by combining domesticated *R. sphaeroides* with *B. subtilis* in an equal volume. The mixed strain (2 mL) was transferred to 100 mL of the degradation medium and cultured for 7 days under different conditions with no inoculated bacteria as a control. The enzymes play a key role in the degradation process of HPAM. Temperature and pH are the main factors affecting the enzyme properties, while the inoculated dosage can directly affect the enzyme dosage. Hence, an orthogonal test[39] of three factors at three different levels was performed to optimize the operation conditions at the given initial pH (6, 7, and 8), temperature (298, 303, and 308 K), and inoculated dosage (1, 2, and 3 mL). The HPAM concentration was measured by the starch-cadmium iodide method at 585 nm,[40,41] and its degradation ratio could be calculated to evaluate the enzymatic degradation performance. Moreover, the degradation ratio of mixed bacteria was compared with the single strain, *R. sphaeroides* and *B. subtilis*, under optimal conditions.

https://doi.org/10.1021/acsomega.2c07380
ACS Omega 2023, 8, 10040−10050

3. RESULTS AND DISCUSSION

3.1. Contribution of Residues to Interaction Energy and The Total Interaction Energy. As can be seen from Figure 1, the residues ILE450, LEU447, TRP328, and ALA195 took part in the hydrophobic actions with HPAM-2 at 298 K. The residues ILE450, ALA332, TRP328, ILE227, and ALA195 produced hydrophobic contacts with HPAM-2 at 303 K. HPAM-2 interacted with residues ILE450, MET449, TRP328, ILE198, and ALA195 by hydrophobic actions at 308 K. These residues contributed to their interaction energies little or even negatively. At the same time, it is also found that the residue LYS96 always contributed the most to the interaction energy at different temperatures. The contribution order of LYS96 to the interaction energy was 303 K > 298 K > 308 K, consistent with the order of total interaction energy, suggesting that the residue LYS96 was the most important residue in the Rh Amidase binding with HPAM-2. From Figure 1d, the total interaction energy was the lowest at 303 K, indicating that the binding of Rh Amidase with HPAM-2 was the best at 303 K.

The three residues, namely, LYS135, ARG136, and ASP113, took part in *B. subtilis* laccase binding with HPAM-3 at 298 K, but only LYS135 was involved in their binding at 303 and 308 K. Thus, it is meaningful to explore the contribution of residues to the interaction energy between *B. subtilis* laccase and HPAM-3 at 298 K. As shown in Figure S4a, the residue LYS135 always contributed the most to the interaction energy, which suggested that LYS135 is the most important residue in the *B. subtilis* laccase binding with HPAM-3. From Figure S4b, the total interaction energy was the lowest at 298 K, indicating that the binding of *B. subtilis* laccase with HPAM-3 was the optimal at 298 K.

3.2. Conformation Transformation. As shown in Figure 2a, the total energies of Rh Amidase-HPAM-2 tended to a constant, indicating that this structure reached equilibrium after MDS optimization. In addition, the total energy of Rh Amidase-HPAM-2 was the largest at 308 K, which further indicated that the stability of this structure is the worst at 308 K. Its total energy had not much difference between 298 and 303 K, and a higher temperature at a certain range was beneficial to the enzymatic reaction. Hence, we selected 303 K as the optimal reaction temperature of Rh Amidase degrading HPAM-2. RMSD is often employed to measure structural stability of the protein backbone atoms. The higher the RMSD value, the worse the stability of the enzyme protein. In order to observe the binding of Rh Amidase to HPAM-2, the variation of RMSD over simulated time was calculated, and the initial conformation was used as a reference, as shown in Figure 2b. The enzyme skeleton vibration was the largest when Rh Amidase was bound to HPAM-2 at 308 K, indicating that their binding was the worst at 308 K. The skeleton vibration of the enzyme between 298 and 303 K was almost the same, and RMSD reached balance earlier at 303 than 298 K when the Rh Amidase was bound with HPAM-2. These further suggested that the binding of Rh Amidase-HPAM-2 was the best at 303 K.

From Figure 3a,b, the conformation of the Rh Amidase-HPAM-2 complex did not change significantly at 298 and 303 K, while the orientation of HPAM-2 changed slightly, indicating that this complex is stable at 298 and 303 K. From Figure 3c, at 308 K, it is worth noting that the enzyme part marked by a dotted line had a larger skeleton fluctuation. This can explain well why the structure of the enzyme acquired the maximum RMSD value when binding to the substrate at 308 K.

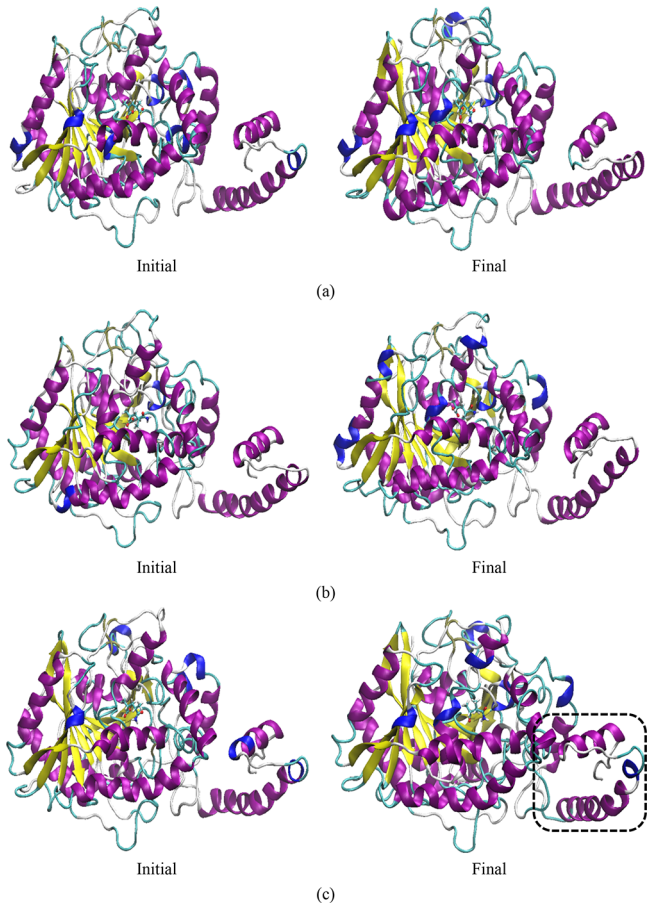

Figure 3. Conformation transformation of Rh Amidase-HPAM-2 at (a) 298, (b) 303, and (c) 308 K. The stick configuration was HPAM-2, and the secondary structure of Rh Amidase was exhibited in a new cartoon pattern. The solvents were not shown for simplicity. Note: the initial and final frames were only analyzed for the 50 ns dynamics trajectory.

As shown in Figure 4a, the total energies of *B. subtilis* laccase-HPAM-3 tended to a constant, indicating that this structure reached equilibrium. Additionally, the total energy of *B. subtilis* laccase-HPAM-3 was the most negative at 298 K, indicating that this structure is the most stable at 298 K. In order to observe the binding of *B. subtilis* laccase-HPAM-3, the variation of RMSD over simulated time was calculated, and the initial conformation was used as a reference, as shown in Figure 4b. From Figure 4b, the enzyme skeleton vibration was the smallest when *B. subtilis* laccase was bound to HPAM-3 at 298 K, which suggested that their binding was the optimal at 298 K. As can be seen from Figure S5a,b, the conformation of the *B. subtilis* laccase-HPAM-3 complex did not change significantly at 298 and 303 K, while the orientation of HPAM-3 changed slightly, indicating that this complex is stable at 298 and 303 K. From Figure S5c, at 308 K, we can find that the HPAM-3 had deviated from the initial docking position of the enzyme, which speculated that it may be due to the larger vibration of the enzyme skeleton, indicating that *B. subtilis* laccase has the worst binding at 308 K.

The higher RMSF reflects the less stability of corresponding individual residues in the enzyme.[42−44] These residues may affect the stability of the enzyme binding to the substrate.

https://doi.org/10.1021/acsomega.2c07380
ACS Omega 2023, 8, 10040−10050

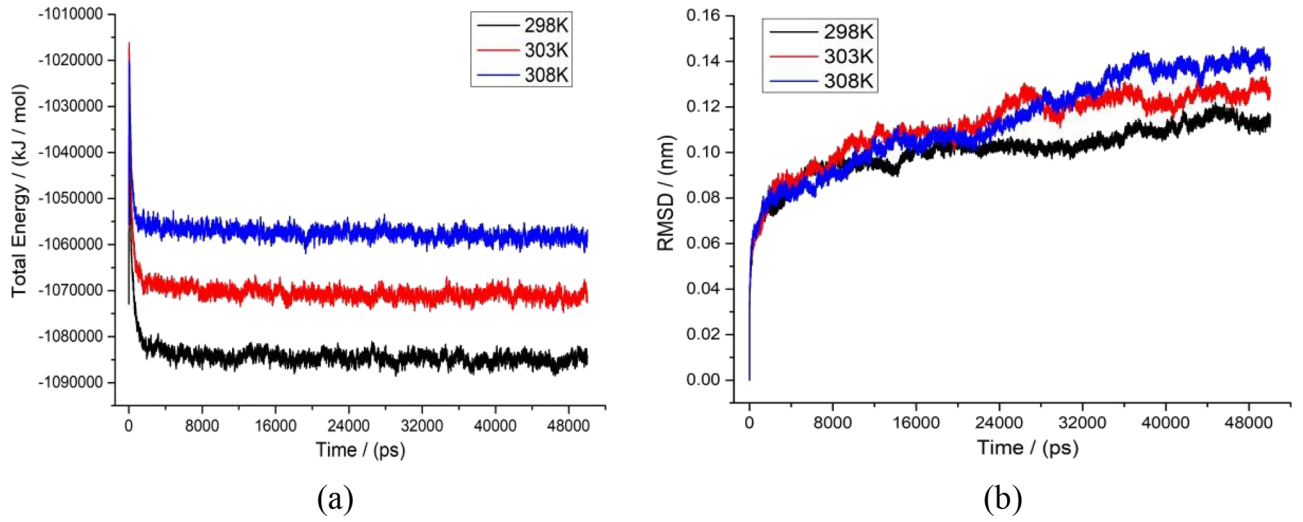

Figure 4. Total energy (a) and RMSD of backbone atoms (b) in *B. subtilis* laccase-HPAM-3 under 298, 303, and 308 K.

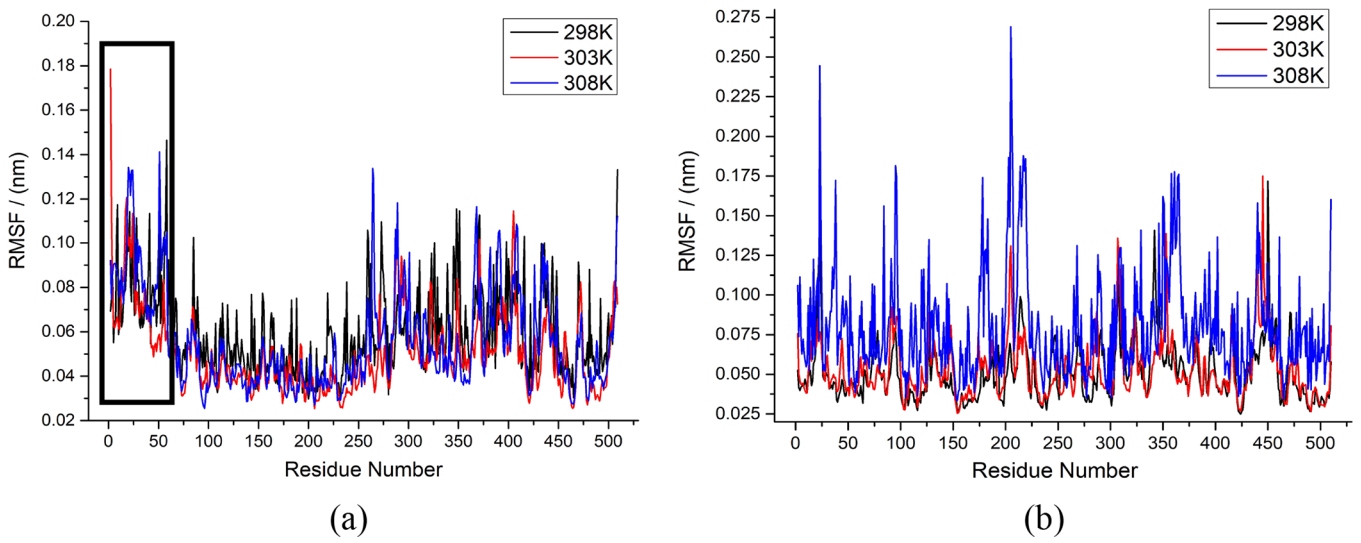

Figure 5. RMSF of enzyme residues in Rh Amidase-HPAM-2 (a) and *B. subtilis* laccase-HPAM-3 (b) at 298, 303, and 308 K.

From what is shown in Figure 5a, the enzyme residue RMSF in Rh Amidase-HPAM-2 had the most fluctuation at 308 K followed by 298 K, while the enzyme residue RMSF in Rh Amidase-HPAM-2 had the smallest fluctuation at 303 K, which further indicated that Rh Amidase binding to HPAM-2 is optimal at 303 K. In addition, at 303 K, Rh Amidase-HPAM-2 enjoyed the highest RMSF only at 0−50 residues of the enzyme, but this value had the smallest variation compared with 298 and 308 K. These indicated that these residues play a dominant role in the stability of Rh Amidase binding to HPAM-2 at 303 K. Locations of 0−50 residues in Rh Amidase are (shown in Figure S6) kept away from the active site of the enzyme, which supposed that these residues only may affect the enzyme binding stability. The calculated enzyme residue RMSF values for *B. subtilis* laccase-HPAM-3 are shown in Figure 5b. From Figure 5b, we can find that the RMSF values of all residues in *B. subtilis* laccase gradually increased with the temperature. Moreover, the RMSF values of all residues for the *B. subtilis* laccase-HPAM-3 at 298 K were the lowest, further indicating that a more stable binding of *B. subtilis* laccase with HPAM-3 was obtained at 298 K.

3.3. Effect of Temperatures on the Binding of the Enzyme to the Substrate. Figure 6a shows that at 298 K, HPAM-2 interacted by forming a hydrogen bond with residues LYS96, SER171, PHE146, GLN192, GLY193, GLY194, and ALA195 in the Rh Amidase. Simultaneously, HPAM-2 formed a water hydrogen bond with a water molecule, so a total of eight hydrogen bonds were formed in Rh Amidase-HPAM-2. Moreover, the four hydrophobic actions of residues TRP328, LEU447, ILE450, and ALA195 with HPAM-2 also could stabilize Rh Amidase-HPAM-2. Lastly, HPAM-2 formed a salt bridge with the LYS96 residue. Figure 6b shows that at 303 K, HPAM-2 interacted by forming hydrogen bonds with residues LYS96, SER171, GLN192, and GLY193 in the Rh Amidase, and the HPAM-2 formed two water hydrogen bonds with two water molecules, so a total of six hydrogen bonds were formed in Rh Amidase-HPAM-2. Furthermore, the seven hydrophobic actions of residues ALA195, ILE227, ALA332, ILE450, and TRP328 with HPAM-2 also could stabilize Rh Amidase-HPAM-2. In the end, HPAM-2 formed an electrostatic interaction with the LYS96 residue. Figure 6c shows that at 308 K, HPAM-2 interacted by forming hydrogen bonds with residues GLN192, GLY193, GLY194, ALA195, and SER171 in

https://doi.org/10.1021/acsomega.2c07380
ACS Omega 2023, 8, 10040−10050

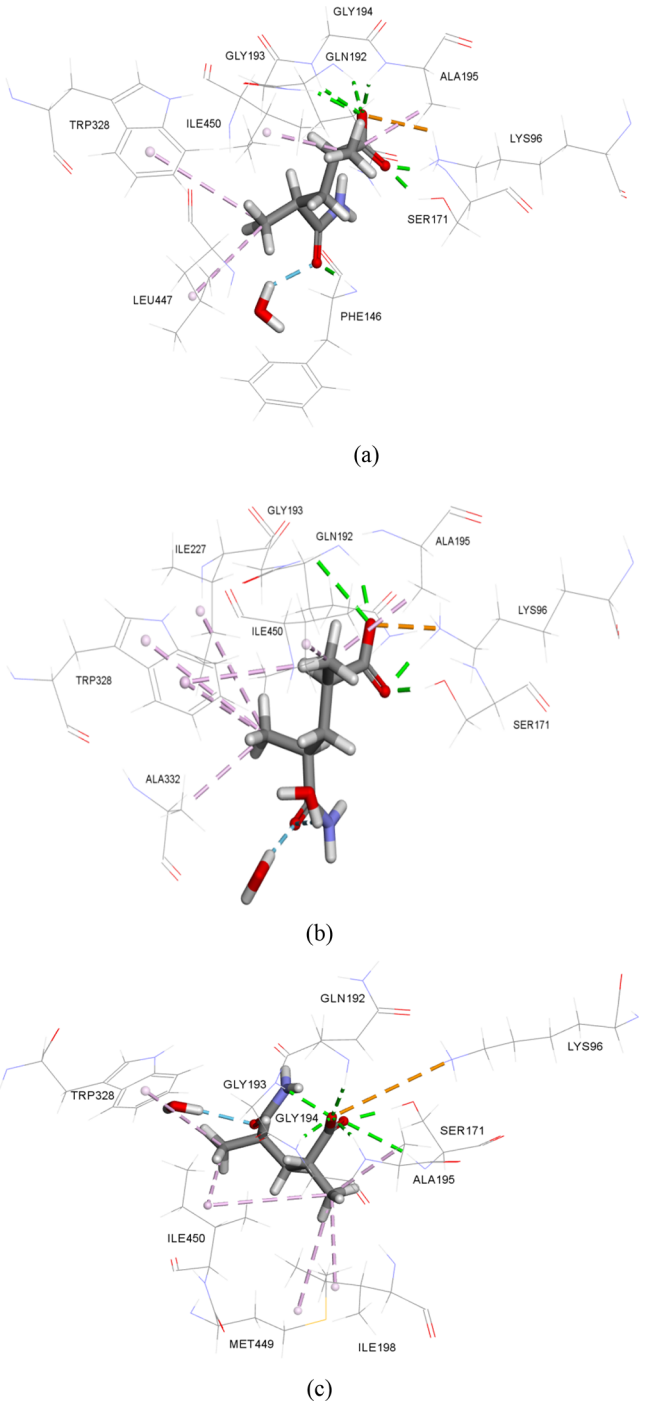

Figure 6. Effect of (a) 298, (b) 303, and (c) 308 K on the binding of Rh Amidase with HPAM-2 (green: hydrogen bond; light blue: water hydrogen bond; pink: hydrophobic; orange: electrostatic or salt bridge). Note: the final frame of a 50 ns NPT MD production was analyzed their interaction.

the Rh Amidase, and the HPAM-2 formed a water hydrogen bond with a water molecule, so a total of seven hydrogen bonds were formed in Rh Amidase-HPAM-2. Additionally, the six hydrophobic actions of residues TRP328, MET449, ILE198, ALA195, and ILE450 with HPAM-2 also contributed to stabilizing Rh Amidase-HPAM-2. Finally, HPAM-2 formed an electrostatic interaction with the LYS96 residue.

The above results are analyzed and summarized in Table 1. From Table 1, we can find that at 298 K, HPAM-2 formed the most number of hydrogen bonds (7) with surrounding residues. Meanwhile, it produced a hydrogen bond and a salt bridge with the LYS96 residue, so Rh Amidase-HPAM-2 was the most stable at 298 K due to a strong hydrogen bond and a salt bridge.

Table 1. Interaction Details of Rh Amidase-HPAM-2 at 298, 303, and 308 K

temperature	interaction residue	type	number
298 K	LYS96, SER171, PHE146, GLN192, GLY193, GLY194, ALA195	hydrogen bond	7
	H_2O	water hydrogen bond	1
	TRP328, LEU447, ILE450, ALA195	hydrophobic	4
	LYS96	salt bridge	1
303 K	LYS96, SER171, GLN192, GLY193	hydrogen bond	4
	H_2O	water hydrogen bond	2
	ALA195, ILE227, ALA332, ILE450, TRP328(3)	hydrophobic	7
	LYS96	electrostatic	1
308 K	GLN192, GLY193, GLY194, ALA195, SER171(2)	hydrogen bond	6
	H_2O	water hydrogen bond	1
	TRP328, MET449, ILE198, ALA195, ILE450(2)	hydrophobic	6
	LYS96	electrostatic	1

As shown in Figure 7a, we can find that at 298 K, HPAM-3 formed six H bonds with residues LYS135, ARG136, and ASP113 in the *B. subtilis* laccase, and it had seven water H bonds with seven water molecules. Moreover, HPAM-3 formed two electrostatic actions with residues LYS135 and ARG136. As shown in Figure 7b, it can be found that at 303 K, the residue LYS135 underwent a H bond and an electrostatic interaction with HPAM-3, and HPAM-3 had 12 water H bonds with 10 water molecules. From Figure 7c, we can find that at 308 K, the HPAM-3 underwent an electrostatic interaction with the residue LYS135 and formed 13 water H bonds with 11 water molecules.

The above analyzed results are listed in Table 2. From Table 2, we can find that at 298 K, HPAM-3 formed the most number of hydrogen bonds (6) and electrostatics (2) with surrounding residues, so *B. subtilis* laccase-HPAM-3 was the most stable at 298 K due to strong hydrogen bonds and electrostatic interactions.

3.4. Cultivation of Two Bacteria. Both *B. subtilis* and *R. sphaeroides* culture results are shown in Figure 8. Figure 9a is an optical microscope image of *R. sphaeroides* using Gram staining, showing that it is a Gram-negative bacterial strain. Figure 9b is an optical microscope image of *B. subtilis* using Gram staining, showing that it is a Gram-positive bacterial strain.

3.5. HPAM Degradation Tests. The used level of the main factors and the L_9 (3^3) matrix were employed to assign experiments, as shown in Tables 3 and 4.

The HPAM degradation ratio was calculated (Table 4). From Table 4, the optimal factor combination $A_3B_2C_2$ was obtained according to the range analysis. Consequently, $A_3B_2C_2$ was selected as the optimal condition to treat 500

https://doi.org/10.1021/acsomega.2c07380
ACS Omega 2023, 8, 10040−10050

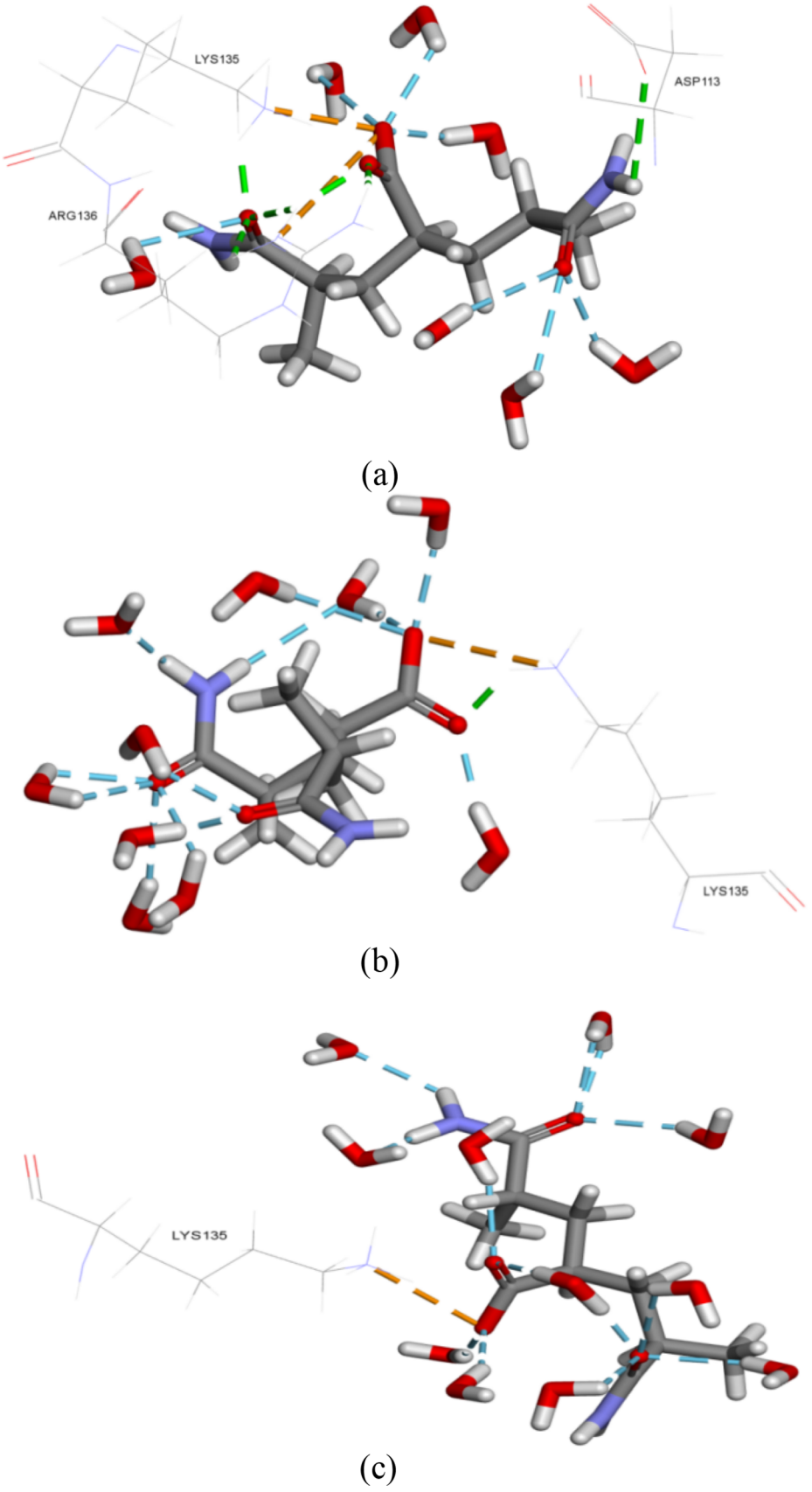

Figure 7. Effect of (a) 298, (b) 303, and (c) 308 K on binding of *B. subtilis* laccase with HPAM-3 (green: hydrogen bond; light blue: water hydrogen bond; orange: electrostatic). Note: the final frame of a 50 ns NPT MD production was analyzed by their interaction.

https://doi.org/10.1021/acsomega.2c07380
ACS Omega 2023, 8, 10040−10050

Table 2. Interaction Details of *B. subtilis* Laccase-HPAM-3 at 298, 303, and 308 K

temperature	interaction residue	type	number
298 K	LYS135, ARG136, ASP113	hydrogen bond	6
	H_2O	water hydrogen bond	7
	LYS135, ARG136	electrostatic	2
303 K	LYS135	hydrogen bond	1
	H_2O	water hydrogen bond	12
	LYS135	electrostatic	1
308 K	LYS135	electrostatic	1
	H_2O	water hydrogen bond	13

Table 3. Factors and Levels of Orthogonal Experiments

factor	*A* (*T*/K)	*B* (initial pH)	*C* (inoculated dosage/mL)
level 1	298	6	1
level 2	303	7	2
level 3	308	8	3

mg/L HPAM wastewater. The corresponding specific optimal conditions were 308 K, initial pH = 7, and an inoculated dosage of 2 mL. These conditions resulted in the HPAM degradation ratio of 39.24%. The effect of operation parameters on the HPAM degradation ratio followed a declining order: temperature > initial pH > inoculated dosage, and temperature was the most important effect factor. A high temperature not only can denature and inactivate the enzymes but also increase energy consumption. Thus, 308 K was chosen as the optimal without considering higher temperatures. Subsequent degradation comparison of mixed bacteria with a single strain was carried out at these optimal conditions. From Figure 10a, the enzymatic reaction rate of *R. sphaeroides* was a little higher than that of *B. subtilis*. This indicated that the activity of amidase secreted by *R. sphaeroides* was better that of *B. subtilis* laccase, and the amide group of HPAM was easier to be degraded by amidase than its carbon chain, which is consistent with experimental results in the literature.[16] As shown in Figure 10b, under the optimal conditions obtained above, the degradation rate of mixed bacteria was higher than that of a single bacterial strain. This is because mixed bacteria can secrete both amidase and laccase. Laccase was more likely to oxidize the carbon chain of HPAM to provide a carbon source when the amide side chain of HPAM was degraded by amidase.

In addition, we can find that HPAM was degraded slowly, and its degradation rate was only 2.58% under natural conditions. This indicated that HPAM can accumulate in sewage for a long time and is difficult to be degraded under natural light irradiation.

3.6. Supposed Codegradation Mechanism by Mixed Bacteria. Previous studies have shown that Rh Amidase was inclined to degrading the short chain of HPAM, and *B. subtilis* laccase accommodated a certain length of HPAM. MD simulation explored the effect of temperature on the stability of enzyme binding to the substrate, and an approximate temperature range was obtained for further experiments. The optimal stability of complexes and enzyme binding to the substrate was obtained by theoretical calculations, while the optimal degradation performance was obtained at 308 K. This may be because a higher temperature, such as 308 K, can enhance the disturbance of complex and enzyme binding to the substrate, promote mass and heat transfer, and thus obtain the optimal degradation performance.

The degradation effect of *R. sphaeroides* was better than that of *B. subtilis*, suggesting that oxidative fracture of the HPAM carbon chain was more difficult than the hydrolysis of its amide group. The degradation effect of mixed bacteria was better than that of a single strain, indicating that the mixed bacteria can simultaneously secrete amidase and laccase; they can jointly degrade HPAM. Figure 11 shows the codegradation mechanism by mixed bacteria, following these two parts: (1) The amide side chain of HPAM was easily hydrolyzed by the

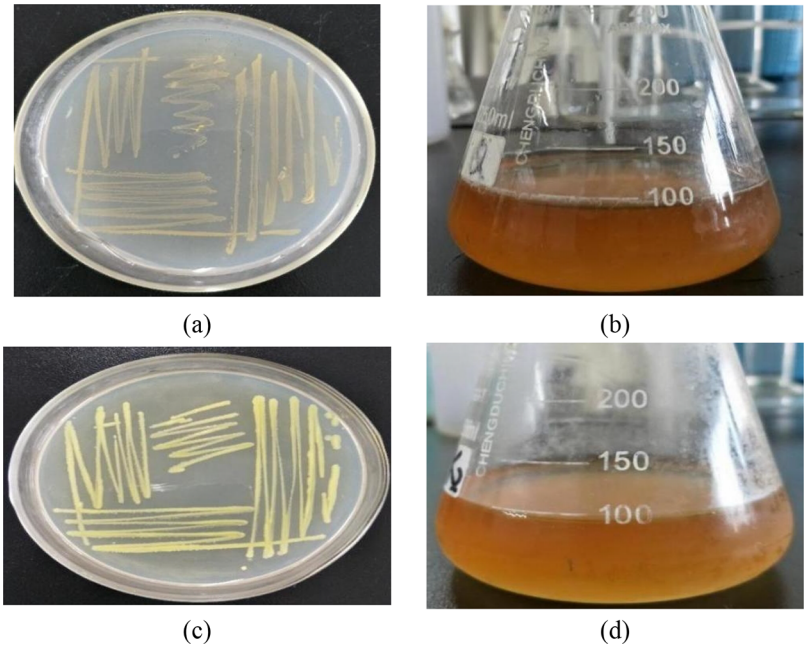

Figure 8. *R. sphaeroides* plate colony morphology (a); *R. sphaeroides* liquid colony morphology (b); *B. subtilis* plate colony morphology (c); *B. subtilis* liquid colony morphology (d).

https://doi.org/10.1021/acsomega.2c07380
ACS Omega 2023, 8, 10040−10050

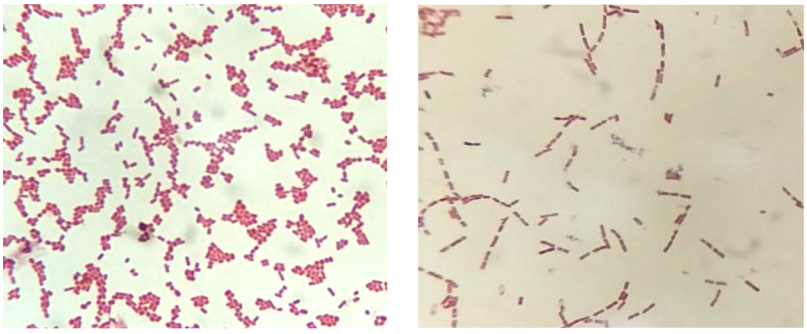

Figure 9. *R. sphaeroides* staining image under light microscopy (a); *B. subtilis* staining image under light microscopy (b).

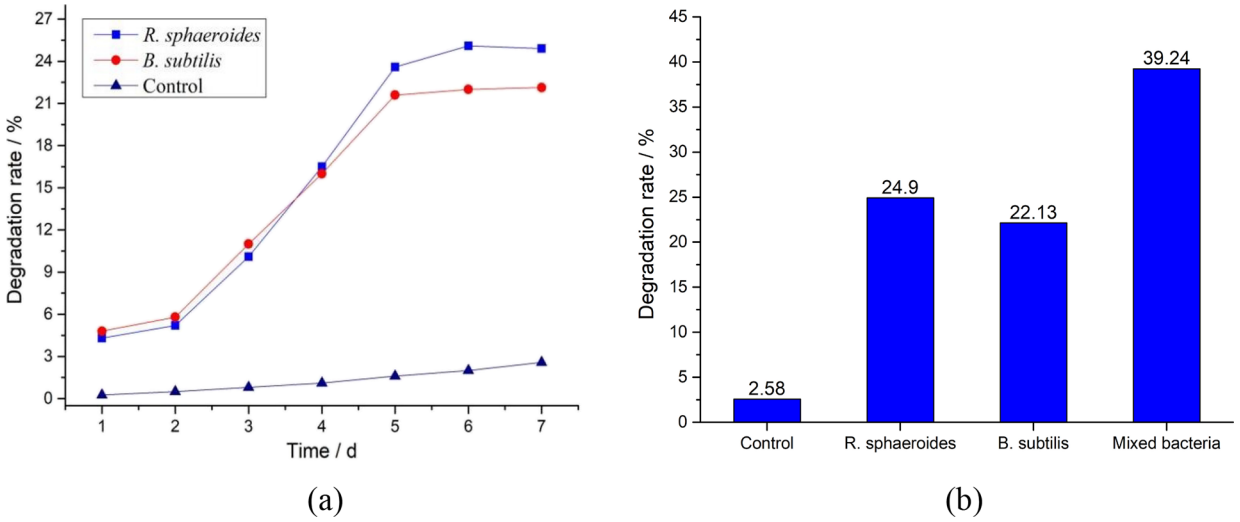

Figure 10. Comparison of degradation between single strain (a) and mixed bacteria (b). Reaction conditions: T = 308 K, initial pH = 7, inoculated dosage = 2 mL, and time = 7days.

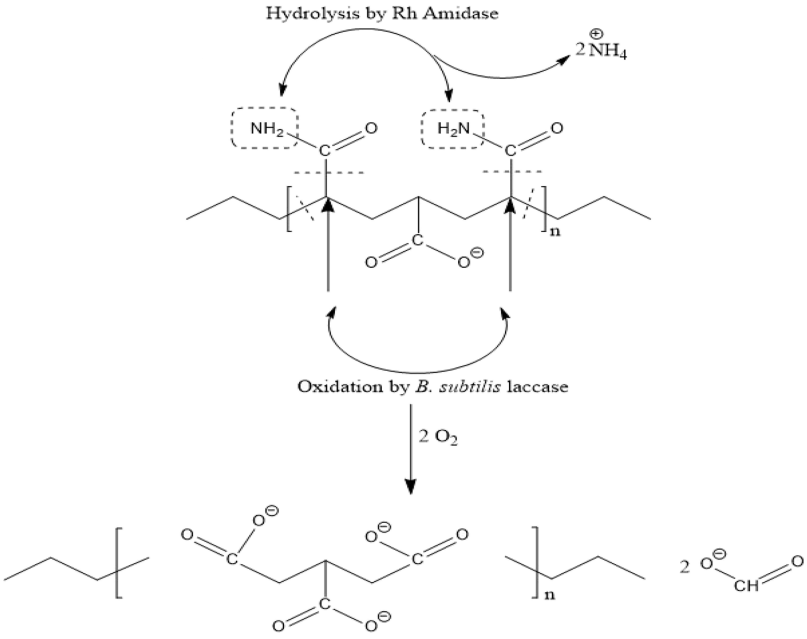

Figure 11. Supposed HPAM codegradation mechanism by mixed bacteria.

amidase secreted by *R. sphaeroides* into NH_4^+ as a nitrogen source. (2) Simultaneously, the carbon chain of HPAM was oxidized and broken by laccase secreted by *B. subtilis* as a carbon source.

https://doi.org/10.1021/acsomega.2c07380
ACS Omega 2023, 8, 10040−10050

Table 4. The Results of Orthogonal Experiments by Mixed Bacteria

factor	A (T/K)	B (initial pH)	C (inoculated dosage/mL)	HPAM degradation ratio /%
1	1 (298 K)	1 (6)	1 (1 mL)	31.20
2	1	2 (7)	2 (2 mL)	33.69
3	1	3 (8)	3 (3 mL)	32.25
4	2 (303 K)	1	2	33.23
5	2	2	3	34.77
6	2	3	1	33.86
7	3 (308 K)	1	3	34.26
8	3	2	1	35.57
9	3	3	2	34.55
K_1	32.38	32.90	33.54	
K_2	33.95	34.68	33.82	
K_3	34.79	33.55	33.76	
R	2.41	1.78	0.28	

4. CONCLUSIONS

The most suitable Rh Amidase-HPAM-2 and *B. subtilis* laccase-HPAM-3 were obtained by docking to further use MDS at 298, 303, and 308 K to evaluate the binding of the enzyme with the substrate and the stability of complexes. The results of MDS analysis show that both Rh Amidase-HPAM-2 and *B. subtilis* laccase-HPAM-3 were the most stable at 298 K. The LYS96 in Rh Amidase-HPAM-2 and LYS135 in *B. subtilis* laccase-HPAM-3 were the key in their binding process at different temperatures. The optimal binding of Rh Amidase-HPAM-2 and *B. subtilis* laccase-HPAM-3 was at 303 and 298 K, respectively. The optimum conditions of mixed bacteria degrading HPAM were 308 K, initial pH = 7, and an inoculated dosage of 2 mL, and the degradation ratio reached 39.24%. The effect of parameters followed a declining order of temperature > initial pH > inoculated dosage. The HPAM codegradation mechanism was supposed by mixed bacteria based on experimental results. The mixed bacteria concurrently secreted both amidase and laccase, and they acted together on HPAM. These data are not only highly valuable and suggest sites for future experimental mutagenesis studies but also a valuable contribution to the scientific literature and further the field understanding of laccase and amidase.

■ ASSOCIATED CONTENT

Supporting Information

The Supporting Information is available free of charge at https://pubs.acs.org/doi/10.1021/acsomega.2c07380.

Relevant calculation details; interaction energy that can evaluate how well the enzyme binds to the substrate; conformational change that can intuitively show the stability of the enzyme binding to the substrate; position of the residues with the greatest fluctuation shown in Rh Amidase (PDF)

■ AUTHOR INFORMATION

Corresponding Author

Fanglue Wang − *School of Bioengineering, Huainan Normal University, Huainan 232038, China;* orcid.org/0000-0002-1795-4543; Email: wangfanglue66@163.com

Authors

Liwen Zhang − *School of Mechanical and Electrical Engineering, Huainan Normal University, Huainan 232038, China*

Dongchen Zhang − *School of Materials Science and Engineering, Anhui University of Science and Technology, Huainan 232001, China*

Xuefeng Wu − *School of Food and Bioengineering, Hefei University of Technology, Hefei 230009, China*

Shengsong Deng − *School of Food and Bioengineering, Hefei University of Technology, Hefei 230009, China*

Complete contact information is available at: https://pubs.acs.org/10.1021/acsomega.2c07380

Notes

The authors declare no competing financial interest.

■ ACKNOWLEDGMENTS

This work was funded by the National Natural Science Foundation of China under grant no. 51274012, the National Natural Science Foundation of China under grant no. 31601465, and the Stable Talent Fund of Huainan Normal University (BSKYQDJ).

■ REFERENCES

(1) Ren, B.; Min, F.; Liu, L.; Chen, J.; Liu, C.; Lv, K. Adsorption of different PAM structural units on kaolinite (001) surface: density functional theory study. *Appl. Surf. Sci.* **2019**, *504*, 144324.

(2) Zou, W.; Zhao, J.; Sun, C. Adsorption of anionic polyacrylamide onto coal and kaolinite calculated from the extended DLVO theory using the van Oss-Chaudhury-Good Theory. *Polymer* **2018**, *10*, 113.

(3) Zou, W.; Cao, Y.; Sun, C. Adsorption of anionic polyacrylamide onto coal and kaolinite: changes of surface free energy components. *Parti. Sci. Technol.* **2017**, *35*, 233−238.

(4) Xia, W.; Li, Y.; Wu, F.; Niu, C. Enhanced flotation selectivity of fine coal from kaolinite by anionic polyacrylamide pre-conditioning. *J. Mol. Liq.* **2021**, *334*, No. 116083.

(5) Lin, Z.; Li, P.; Hou, D.; Kuang, Y.; Wang, G. Aggregation mechanism of particles: Effect of Ca^{2+} and polyacrylamide on coagulation and flocculation of coal slime water containing illite. *Minerals.* **2017**, *7*, 30.

(6) Castro, S.; Laskowski, J. S. Depressing effect of flocculants on molybdenite flotation. *Miner. Eng.* **2015**, *74*, 13−19.

(7) Hu, H.; Liu, J.-F.; Li, C.-Y.; Yang, S.-Z.; Gu, J.-D.; Mu, B.-Z. Anaerobic biodegradation of partially hydrolyzed polyacrylamide in long-term methanogenic enrichment cultures from production water of oil reservoirs. *Biodegadation.* **2018**, *29*, 233−243.

(8) Xiong, B.; Purswani, P.; Pawlik, T.; Samineni, L.; Karpyn, Z.; Zydney, A.; Kumar, M. Mechanical degradation of polyacrylamide at ultra high deformation rates during hydraulic fracturing. *Environ. Sci.: Water Res. Technol.* **2020**, *6*, 166−172.

(9) Yang, Y.; Xin, L.; Zhou, C.; Xiong, W.; Zeng, G.; Huang, D.; Zhang, C.; Wang, W.; Song, B.; Tang, X.; et al. Recent advances in application of graphitic carbon nitride-based catalysts for degrading organic contaminants in water through advanced oxidation processes beyond photocatalysis: A critical review. *Water Res.* **2020**, *184*, No. 116200.

(10) Wang, W.; Niu, Q.; Zeng, G.; Zhang, C.; Huang, D.; Shao, B.; Zhou, C.; Yang, Y.; Liu, Y.; Guo, H.; Xiong, W.; Lei, L.; Liu, S.; Yi, H.; Chen, S.; Tang, X. 1D porous tubular g-C_3N_4 capture black phosphorus quantum dots as 1D/0D metal-free photocatalysts for oxytetracycline hydrochloride degradation and hexavalent chromium reduction. *Appl. Catal. B* **2020**, *273*, No. 119051.

(11) Zhao, L.; Bao, M.; Yan, M.; Lu, J. Kinetics and thermodynamics of biodegradation of hydrolyzed polyacrylamide under anaerobic and aerobic conditions. *Bioresour. Technol.* **2016**, *216*, 95−104.

(12) Zhang, C.; Zhao, L.; Bao, M.; Lu, J. Potential of hydrolyzed polyacrylamide biodegradation to final products through regulating its own nitrogen transformation in different dissolved oxygen systems. *Bioresour. Technol.* **2018**, *256*, 61−68.
(13) Wen, Q.; Chen, Z.; Zhao, Y.; Zhang, H.; Feng, Y. Biodegradation of polyacrylamide by bacteria isolated from activated sludge and oil-contaminated soil. *J. Hazard. Mater.* **2010**, *175*, 955−959.
(14) Bao, M.; Chen, Q.; Li, Y.; Jiang, G. Biodegradation of partially hydrolyzed polyacrylamide by bacteria isolated from production water after polymer flooding in an oil field. *J. Hazard. Mater.* **2010**, *184*, 105−110.
(15) Nyyssölä, A.; Ahlgren, J. Microbial degradation of polyacrylamide and the deamination product polyacrylate. *Int. Biodeterior. Biodegrad.* **2019**, *139*, 24−33.
(16) Sang, G.; Pi, Y.; Bao, M.; Li, Y.; Lu, J. Biodegradation for hydrolyzed polyacrylamide in the anaerobic baffled reactor combined aeration tank. *Ecol. Eng.* **2015**, *84*, 121−127.
(17) Zhao, L.; Song, T.; Han, D.; Bao, M.; Lu, J. Hydrolyzed polyacrylamide biotransformation in an up-flow anaerobic sludge blanket reactor system: Key enzymes, functional microorganisms, and biodegradation mechanisms. *Bioprocess Biosyst. Eng.* **2019**, *42*, 941−951.
(18) Song, T.; Li, S.; Ding, W.; Li, H.; Bao, M.; Li, Y. Biodegradation of hydrolyzed polyacrylamide by the combined expanded granular sludge bed reactor-aerobic biofilm reactor biosystem and key microorganisms involved in this bioprocess. *Bioresour. Technol.* **2018**, *263*, 153−162.
(19) Tian, J.; Wang, P.; Gao, S.; Chu, X.; Wu, N.; Fan, Y. Enhanced thermostability of methyl parathion hydrolase from *Ochrobactrum sp.* M231 by rational engineering of a glycine to proline mutation. *FEBS J.* **2010**, *277*, 4901−4908.
(20) Wang, F.; Zhang, D.; Wu, X.; Deng, S. Biodegradation of anionic polyacrylamide mediated by laccase and amidase: Docking, virtual mutation based on affinity and DFT study. *New J. Chem.* **2021**, *45*, 14554−14562.
(21) Zhao, X.; Song, L.; Fu, J.; Tang, P.; Liu, F. Experimental and DFT investigation of surface degradation of polyvinylidene fluoride membrane in alkaline solution. *Surf. Sci.* **2011**, *605*, 1005−1015.
(22) Ohtaki, A.; Murata, K.; Sato, Y.; Noguchi, K.; Miyatake, H.; Dohmae, N.; Yamada, K.; Yohda, M.; Odaka, M. Structure and characterization of amidase from *Rhodococcus sp*. N-771: Insight into the molecular mechanism of substrate recognition. *Biochim. Biophys. Acta* **2010**, *1804*, 184−192.
(23) Enguita, F. J.; Martins, L. O.; Henriques, A. O.; Carrondo, M. A. Crystal structure of a bacterial endospore coat component. *J. Biol. Chem.* **2003**, *278*, 19416−19425.
(24) Zhang, Y.; Zeng, Z.; Zeng, G.; Liu, X.; Chen, M.; Liu, L.; Liu, Z.; Xie, G. Enzyme-substrate binding landscapes in the process of nitrile biodegradation mediated by nitrile hydratase and amidase. *Appl. Biochem. Biotechnol.* **2013**, *170*, 1614−1623.
(25) Singh, D.; Sharma, K. K.; Jacob, S.; Gakhar, S. K. Molecular docking of laccase protein from *Bacillus Safensis* DSKK5 isolated from earthworm gut: A novel method to study dye decolorization potential. *Water Air Soil Pollu.* **2014**, *225*, 2175.
(26) Tu, M.; Wang, C.; Chen, C.; Zhang, R.; Liu, H.; Lu, W.; Jiang, L.; Du, M. Identification of a novel ACE-inhibitory peptide from casein and evaluation of the inhibitory mechanisms. *Food Chem.* **2018**, *256*, 98−104.
(27) Liu, Z.; Shao, B.; Zeng, G.; Chen, M.; Li, Z.; Liu, Y.; Jiang, Y.; Zhong, H.; Liu, Y.; Yan, M. Effects of rhamnolipids on the removal of 2,4,2,4-tetrabrominated biphenyl ether (BDE-47) by *Phanerochaete chrysosporium* analyzed with a combined approach of experiments and molecular docking. *Chemosphere* **2018**, *210*, 922−930.
(28) Tu, M.; Liu, H.; Zhang, R.; Chen, H.; Mao, F.; Cheng, S.; Lu, W.; Du, M. Analysis and evaluation of the inhibitory mechanism of a novel angiotensin-I-converting enzyme inhibitory peptide derived from casein hydrolysate. *J. Agric. Food Chem.* **2018**, *66*, 4139−4144.
(29) Chen, M.; Zeng, G.; Lai, C.; Li, J.; Xu, P.; Wu, H. Molecular basis of laccase bound to lignin: insight from comparative studies on the interaction of *Trametes versicolor* laccase with various lignin model compounds. *RSC Adv.* **2015**, *5*, 52307−52313.
(30) Liu, Y.; Liu, Z.; Zeng, G.; Chen, M.; Jiang, Y.; Shao, B.; Li, Z.; Liu, Y. Effect of surfactants on the interaction of phenol with laccase: Molecular docking and molecular dynamics simulation studies. *J. Hazard. Mater.* **2018**, *357*, 10−18.
(31) Purmonen, M.; Valjakka, J.; Takkinen, K.; Laitinen, T.; Rouvinen, J. Molecular dynamics studies on the thermostability of family II xylanases. *Protein Eng., Des. Sel.* **2007**, *20*, 551−559.
(32) Liu, J.; Yu, H.; Shen, Z. Insights into thermal stability of thermophilic nitrile hydratases by molecular dynamics simulation. *J. Mol. Graphics Moddel.* **2009**, *27*, 529−535.
(33) Berendsen, H.; Van der spoel, D.; Van drunen, R. GROMACS: A message-passing parallel molecular dynamics implementation. *Comput. Phys. Commun.* **1995**, *91*, 43−56.
(34) Yong, D.; Wu, C.; Chowdhury, S.; Lee, M.; Xiong, G.; Zhang, W.; Yang, R.; Cieplak, P.; Luo, R.; Lee, T.; et al. A point-charge force field for molecular mechanics simulations of proteins based on condensed-phase quantum mechanical calculations. *J. Comput. Chem.* **2003**, *24*, 1999−2012.
(35) Berendsen, H. J.; Postma, J. P.; Van Gunsteren, W. F.; Hermans, J. Interaction models for water in relation to protein hydration. In *Intermolecular forces*. Springer, Dordrecht, 1981; pp. 331−342, DOI: 10.1007/978-94-015-7658-1_21
(36) Essmann, U.; Perera, L.; Berkowitz, M. L.; Darden, T.; Lee, H.; Pedersen, L. G. A smooth Particle Mesh Ewald method. *J. Chem. Phys.* **1995**, *103*, 8577−8593.
(37) Berendsen, H. J. C. Transport properties computed by linear response through weak coupling to a bath. In *Computer Simulation in Materials Science*. Springer, Dordrecht, 1991; pp. 139−155, DOI: 10.1007/978-94-011-3546-7_7
(38) Berendsen, H. J.; Postma, J. V.; Van Gunsteren, W. F.; DiNola, A. R.; Haak, J. R. Molecular dynamics with coupling to an external bath. *J. Chem. Phys.* **1984**, *81*, 3684−3690.
(39) Pi, Y.; Zheng, Z.; Bao, M.; Li, Y.; Zhou, Y.; Sang, G. Treatment of partially hydrolyzed polyacrylamide wastewater by combined Fenton oxidation and anaerobic biological processes. *Chem. Eng. J.* **2015**, *273*, 1−6.
(40) Yan, M.; Zhao, L.; Bao, M.; Lu, J. Hydrolyzed polyacrylamide biodegradation and mechanism in sequencing batch biofilm reactor. *Bioresour. Technol.* **2016**, *207*, 315−321.
(41) Zhao, L.; Zhang, C.; Bao, M.; Lu, J. Effects of different electron acceptors on the methanogenesis of hydrolyzed polyacrylamide biodegradation in anaerobic activated sludge systems. *Bioresour. Technol.* **2018**, *247*, 759−768.
(42) Fujiwara, R.; Nakajima, M.; Yamamoto, T.; Nagao, H.; Yokoi, T. In silico and in vitro approaches to elucidate the thermal stability of human UDP-glucurono-syltransferase (UGT) 1A9. *Drug Metab. Pharmacokinet.* **2009**, *24*, 235−244.
(43) Yan, M. C.; Sha, Y.; Wang, J.; Xiong, X. Q.; Ren, J. H.; Cheng, M. S. Molecular dynamics simulations of HIV-1 protease monomer: assembly of N-terminus and C-terminus into beta-sheet in water solution. *Proteins: Struct., Funct., Bioinf.* **2008**, *70*, 731−738.
(44) Sun, H.; Jiang, Y. J.; Yu, Q. S.; Luo, C. C.; Zou, J. W. Effect of mutation K85R on GSK-3beta: Molecular dynamics simulation. *Biochem. Biophys. Res. Commun.* **2008**, *377*, 962−965.

https://doi.org/10.1021/acsomega.2c07380
ACS Omega 2023, 8, 10040−10050